HIGH-RESOLUTION MULTI-BEAM FOCUSSED SIDE SCAN SONAR

Lloyd C. Huff

National Ocean Service
Rockville, Maryland, 20852 USA

1. SUMMARY

A category of side scan sonar has come to fruition in the civil marine community which greatly extends the performance envelope beyond that of a standard single-beam unfocussed side scan sonar. The system uses phased array technology to increase the allowable rate of high-resolution area coverage. Images of natural and manmade targets obtained with a prototype of this newly available category of system are presented. Remarkedly clear details of complex seabed scenes can be captured while towing at speeds up to 5 m/s.

2. INTRODUCTION

In side scan sonar, the received signals following each short transmit pulse are sampled and recorded as a relatively long-time-series. This provides information related to the magnitude of backscatter from across a wide swath of the seabed (Geyer 1992). Accumulation of such data from successive pings can produce an image of the spatial variations of seabed backscatter as the side scan sonar moves in the alongtrack direction. The clarity and cohesiveness of the image depend on the inherent resolution of the spatial sampling/measurement process, the pulse repetition rate, the tow speed, and the short-term stability of the towfish trajectory.

Since the 1960's when commercial implementation of side scan sonar began, designers and users have pressed for higher-and-higher resolution and higher tow speeds. Based on the titles of papers presented at this International Conference on Acoustic Classification and Mapping of the Seabed, the pursuit for increased resolution is ongoing.

Commercial systems have reached the point where crosstrack resolution is about an order of magnitude better than alongtrack resolution. Crosstrack resolution is inversely related to the length of the transmit pulse (Mazel 1985), but the achieved resolution also depends on the particular combination of transducer bandwidth, post-detection bandwidth, and presentation medium. Side scan sonars use long, narrow transducers mounted such that the beam is wide in the vertical plane and narrow in the alongtrack direction of the horizontal plane (Flemming 1976). Since the 1960's, significant improvements in alongtrack resolution have been achieved by increasing the "length" of the transducers. One can increase the "length" of a transducer by increasing the physical dimension of the transducer and/or reducing the acoustic wavelength (Urick 1983). Side scan sonars are typically towed at 2 m/s or less because the image quality can seriously suffer due to spatial aliasing if the towfish advance between pulses exceeds the alongtrack resolution of the system. The speed at which this becomes a problem depends on the crosstrack dimension of the image area. In other words, one must avoid the operating condition where the time required for the acoustic energy to traverse the round-trip distance between the transducer and the maximum crosstrack range exceeds the time for the side scan sonar to advance the distance equivalent to the system's alongtrack footprint (Lenhardt 1974).

Conventional side scan sonar designs using a single unfocussed transducer per side, inherently have an undesirable low limit for high-resolution area coverage. To increase tow speed, the crosstrack dimension of the image area must be reduced or the alongtrack resolution of the system must be degraded. It is, however, possible to achieve considerably greater rates of high-resolution area coverage by changing the transducer design from the conventional single element to that of a multiple element array and employing focussed array techniques (Fox and Denbigh 1983).

3. DISCUSSON

A prototype system, specifically designed for a high rate of high-resolution area coverage, was developed by Klein Associates Inc. of Salem, New Hampshire, for the National Ocean Service (Huff and Weintroub 1990). The images presented in this paper were obtained with the prototype system. The basic theory of array focussing, first published 50 years ago (Schelnukoff 1943), is well represented in the open technical literature to date, and is undoubtably a topic that will continue to appear in new forums under new authorship.

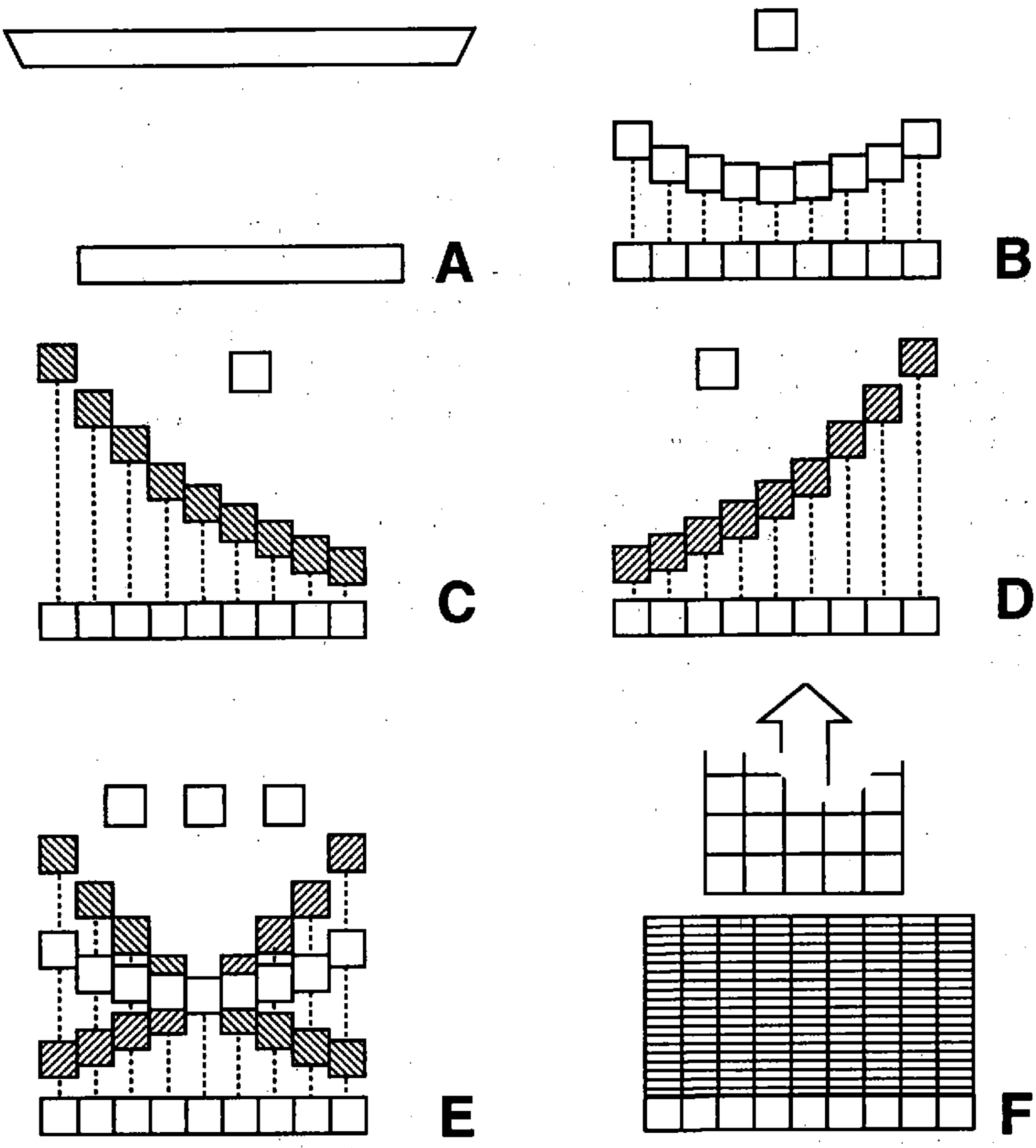

Figure 1. Representation of Array Focussing Using Mechanical Analog: (A) Unfocussed; (B, C, and D) Focus on one cell; (E) Simultaneous focus on three cells; (F) Simultaneous focus on five cells at time varing range.

Using the rude representations of figure 1, it is possible to sufficiently illustrate the salient points of focussed arrays that are relevant to this paper.

Section A of figure 1 depicts an alongtrack resolution cell associated with a single continuous transducer. The rectangle represents the transducer and the polygon above it represents a resolution cell located somewhere at a considerable distance in the crosstrack direction. To a first approximation, the alongtrack resolution cell from a single transducer will always be equal to or greater than the alongtrack dimension of the transducer (Macovski 1979). The ratio of alongtrack resolution cell dimension to transducer alongtrack dimension increases with crosstrack distance from the transducer.

There are designs where array focussing is fixed and involves physically displacing elements of the array or superimposing an acoustic lens over the face of the transducer. Focussing, as discussed herein, is dynamic and involves modifying the electrical phasing of the transducer output signals. However, the modifications made to the electrical phasing of the transducer outputs are such that the signals closely approximate the phasing that would have been experienced if each of the transducers had actually been physically displaced from its "unfocussed" position to its "focussed" position. At the "focussed" positions, the several individual transducers would simultaneously experience a particular constant phase front of acoustic signals radiating outward from the centrally located resolution cell shown above the transducer array.

Section B of figure 1 depicts a centrally located alongtrack resolution cell associated with a focussed array whose aggregate alongtrack dimension is equal to that of the single transducer in section A. For discussion, the individual transducers in the array appear in their "focussed" and "unfocussed" positions. In this case, the resolution cell alongtrack dimension must be equal to or greater than the alongtrack dimension of an individual transducer within the array.

Section C of figure 1 depicts a noncentrally located alongtrack resolution cell. The "focussed" positions of the individual transducers differ from those in section B, as required to position the transducers for simultaneous expressions of constant acoustic phase from the noncentrally located resolution cell.

Section D of figure 1 depicts a noncentrally located alongtrack resolution cell positioned as the mirror image of section C. As one should expect, the "focussed" positions of the individual transducers also mirror those of section C.

In the prototype system, dynamic focussing is accomplished by electrically adjusting the phasing of the transducer signal outputs. Therefore, it is possible to simultaneously focus the array on more than one resolution cell at any time and on different resolution cells at different times. This is depicted in section E of figure 1 and is accomplished by modifying the output signal from each transducer with several differing phasings, one for each desired focussed resolution cell.

The dynamic focussing technique may be extended to provide resolution cells that are contiguous or overlapping in the alongtrack direction (Weintroub and Huff 1992). Section F of figure 1 depicts the case of contiguous resolution cells. The phasing of each individual transducer's received signals can be adjusted to maintain five adjacent resolution cells whose centers move in the crosstrack direction at one-half the propagation speed of the transmit pulse. This assures that the array remains focussed on the moving backscatter footprint associated with the received signals.

The actual image quality from a focussed array depends on the number and alongtrack dimension of the individual transducers, the acoustic frequency, and the degree to which the resolution cells overlap in the alongtrack direction. The prototype system operated at an acoustic frequency of approximately 390 kHz, using 14 individual transducers, each 10 cm long (Huff and Weintroub 1990).

Having given a simplified explanation of the mechanism of focussing, it remains to explain the advantages of focussing. The first advantage is the reduced alongtrack dimension of the resolution cells (Huff and Weintroub 1991). The second advantage is the increase in allowable alongtrack speed. This advantage stems from the ability to simultaneously focus the array on several alongtrack resolution cells. Without this ability, the maximum distance the towfish could advance alongtrack between successive transmit pulses would be limited to the alongtrack dimension of the resolution cell. With "N" alongtrack resolution cells being imaged simultaneously, the towfish is allowed to advance "N times" the alongtrack dimension of an individual resolution cell between successive transmit pulses. The prototype system images five resolution cells in parallel and has a maximum alongtrack speed of 5 m/s. Data from the five beams are digitally recorded with 14-bit resolution at a 12 kHz sample rate. Real-time images are also recorded on a high resolution thermal recorder at 8 pixels per mm with a total of 1652 pixels allocated to represent the full scale crosstrack slant range.

The third advantage of focussing is the improved quality of the seabed images. By adjusting the phasing of the individual transducer output signals, the acoustic energy from any given resolution cell is effectively constructively summed and the acoustic energy from regions separated from the resolution cell is destructively summed. Consequently, the energy used to compose a resolution cell within the seabed image preferentially represents energy from that resolution cell compared to energy from all other potential sources of energy.

At the operator's option, the five parallel resolution cells of the prototype system may be set to overlap thereby producing a slight correlation between alongtrack resolution cells. The images in figures 3 and 4 were obtained at 5 m/s with a 20 cm center-to-center separation between adjacent resolution cells which provides no alongtrack beam-to-beam overlap. The images in all other figures herein were obtained at 3 m/s with 12 cm center-to-center beam separations.

4. RESULTS

The prototype system has been operated in the classic towed mode and in a shallow-water, hull-mounted mode. In the towed mode, the length of the tow cable is adjusted to fly the towfish above the general seabed at 10 to 20 percent of the system's 150 m maximum crosstrack range. In the hull-mounted mode, the system has been operated when the under-keel depth was 2 to 30 m. Figure 2 illustrates the system

Figure 2. Prototype system strapped to the bottom of small hydrographic launch: showing straps, mating saddle, and starboard transducer.

in the hull-mounted mode. It was temporarily attached onto the bottom of a small hydrographic launch. The images in figures 3 and 4 were obtained in the towed mode and all other seabed images herein were obtained in the shallow-water, hull-mounted mode.

The images in this paper are photographic reproductions of digital data and displayed in 16-shades-of-gray on a video monitor. The translation of 14-bit resolution recorded data into 16-shades-of-gray for display on a video monitor is made in post-survey processing and can be customized for each scene, based on the total variations in backscatter amplitudes or the amplitude of a particular feature. The particular combination of video monitor and camera lens used to reproduce the images in this paper introduced a slight distortion. The detectable curvature along the perimeter of the images is an artifact of the photographic process and not a characteristic of the sonar.

Figure 3 is divided into five sections. The basic image data underlying this figure were obtained with the high-resolution multi-beam focussed sonar from a field of sand waves off the southern coast of Devon, England. The figure illustrates the impact of spatial aliasing which might occur when the alongtrack speed of a side scan sonar exceeds the allowable maximum.

Panel A repeats data samples from beam 1 five times in succession. Panel B repeats data samples from beam 1 three times coupled with two successive repeats of beam 2. Panel C is comprised of two repeats of beam 1, two repeats of beam 2, and one repeat of beam 3. Panel D is comprised of two repeats of beam 1 plus one repeat of beams 2, 3, and 4. Panel E is comprised of one repeat of beams 1, 2, 3, 4, and 5. This scheme maintained a constant alongtrack/crosstrack aspect ratio in the various panels. In each panel, the repetition of the beam data occurs only in the alongtrack direction. The data from each beam are allowed to vary naturally in the crosstrack direction. This disassembly and reassembly of the image reduces the image quality when less than the full set of beam data are employed. In the limit when only the data from a single beam are used for the reassembly, the basic orientation of the sand wave crests in the upper half of the image appears to shift by 90 degrees. This case of single-beam image reassembly simulates spatial aliasing that may occur if there are alongtrack gaps in a side scan sonar's bottom coverage due to exceeding that system's maximum rate for high-resolution area coverage.

Figure 4 also contains five panels and depicts the same field of sand waves as the previous figure. Here, the panel to panel differences in the images are due to

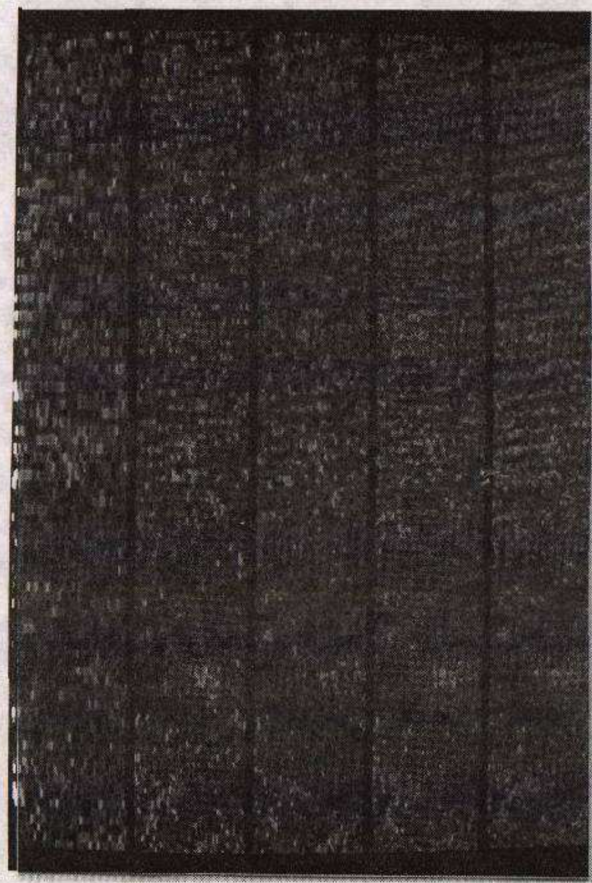

Figure 3. Reassembled images.

Subsets:
(A) Beam 1
(B) Beam 1 & 2
(C) Beam 1, 2, & 3
(D) Beam 1,2, 3, & 4
(E) Beam 1, 2, 3, 4, & 5

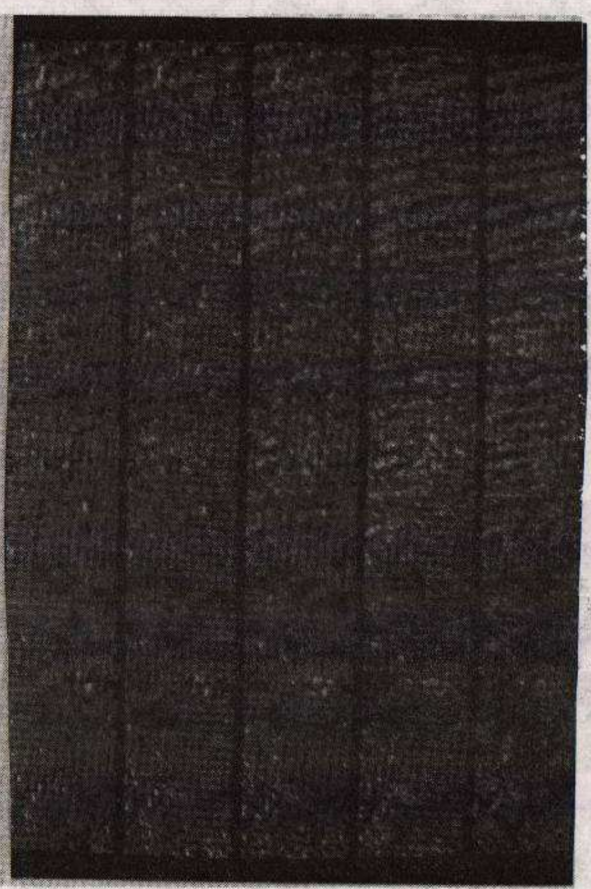

Figure 4. Reassembled images

Boxcar filter width
(A) 5 Beams
(B) 4 Beams
(C) 3 Beams
(D) 2 Beams
(E) 1 Beam

variations in post-survey averaging. Panels A, B, C, D,and E present cases where images, reassembled as in Panel E of figure 3, have been subjected to a boxcar filter in the alongtrack direction, respectively spanning 1, 2, 3, 4, and 5 adjacent beams. There are differences between the images in the five panels. Fine alongtrack details in panel E progressively disappear as the filter width increases.

Figures 3 and 4, taken together, demonstrate the necessity and advantage of a high-resolution multi-beam focussed system in conjunction with high towing speeds while in pursuit of increased rates of high-resolution area coverage.

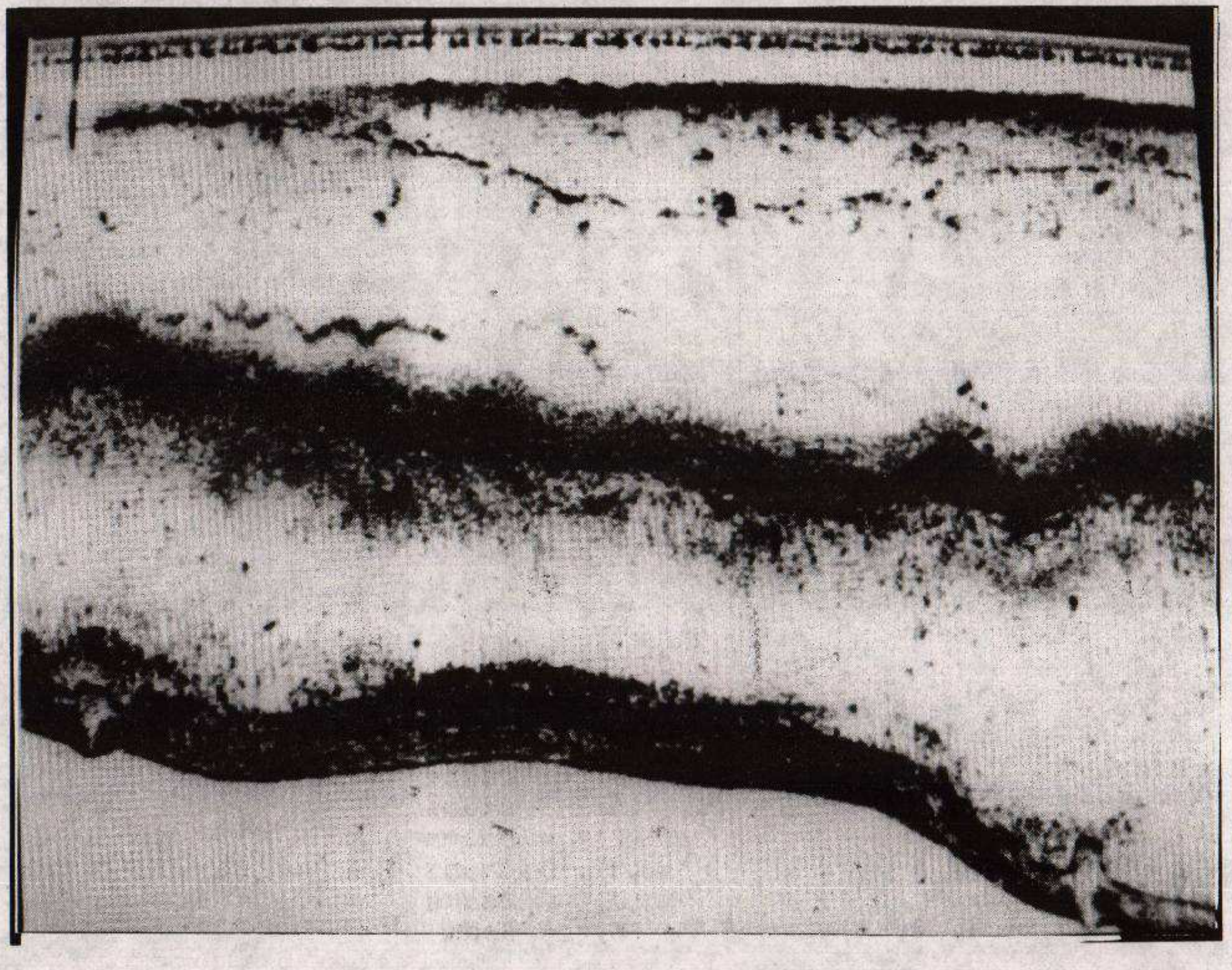

Figure 5. Side Scan Sonar Image of Shoreline

Figure 5 presents an unusual aspect of side scan sonar imagery in that one of the principal features in the image is the shoreline. The image is 86.4 m slant range by 245 m alongtrack. Some of the low amplitude features were sacrificed in the reproduction in favor of presenting details within the areas of large amplitude backscatter.

The narrow, dark band in the upper portion of the figure is due to signals returned from the bottom of the small hydrographic launch to which the system was hull-mounted. Going toward increasing slant range, there is the water column followed by the first seabed encounter of the transmitted pulse. The scalloped pattern on either side of a region of low amplitude returns are the results of recent dredging operations. After a narrow region of low backscatter, there is a wide, dark band which represents the historic edge of the flow channel where the backscatter is enhanced due to bottom slope. Next, there is a wide region of low backscatter followed by a second wide, dark band. The limit of the final dark band in the crosstrack direction represents the intersection of the air/water interface with a sand beach. There is noticeable structure within the final dark band which represents previous locations of the air/water/sand juncture. Toward both the lower left and right edges of the image there is a singular feature where the air/water/sand juncture juts out in the direction of increased crosstrack distance. At each of these points, the final dark band is modified. There are two storm drains whose discharge runs down the sand beach into the waterway. Locally the sand has been eroded and redistributed. The image reflects the resultant local changes in bottom slope and not a change in bottom material.

The image in figure 6 is 36.4 m slant range by 245 m alongtrack and was taken with approximately 18 m of water under the keel. It contains a shadow which clearly demonstrates the remarkable alongtrack resolution of the focussed side scan sonar. The image also contains returns from within the water column, long wavelength sand waves, and the anchor chain of a large tanker. The anchor is located beyond the left side of the image. In the center of the image near the first bottom return, there is a large feature somewhat like an inverted letter "U." On inspection, the left half of the feature contains a highlight from the anchor chain followed immediately by a shadow. Near the upper turning point of the feature, the shadow and highlight diverge. At that point, the mooring chain rises from the bottom on its way to the tanker's bow hawser pipe. The alongtrack resolution cell of the multi-beam focussed side scan sonar has sufficient spatial discrimination to allow the shadow of the chain's links to be distinguished across the image. A portion of the shadow

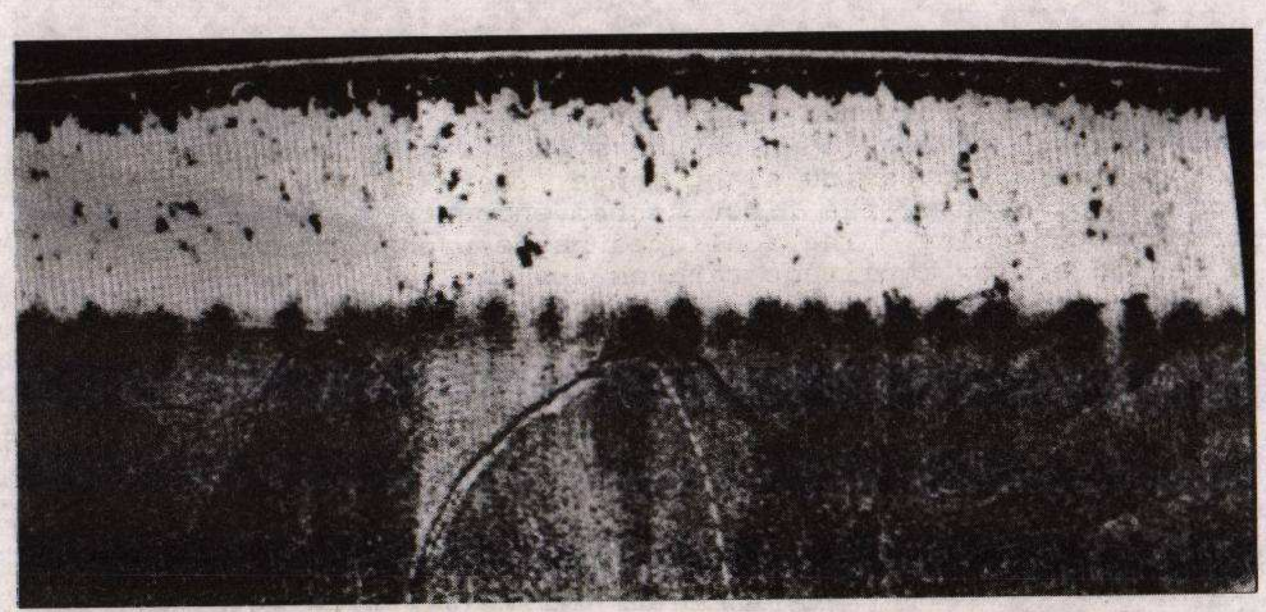

Figure 6. Side Scan Sonar Image of chain on bottom and rising into the water column.

is actually dashed, as the projected width of the chain varies between 5 and 15 cm, due to the orthogonal aspects of adjacent chain links.

The image in figure 7 is 57.6 m slant range by 245 m alongtrack. It contains a ship's wake, long wavelength sand waves, and a family of bottom scars resulting from interaction between the sediment and an anchor chain as the moored vessel moved under the combined forces of wind, waves, and currents. The right half of the image is devoid of the long wavelength sand waves that dominate the left half of the image. There is a dominate loop-to-loop feature with a highlight and an immediate shadow which starts in the center of the image near the first bottom return. It continues toward the lower right corner of the image where it divides into two branches. The upper of the two branches connects to a fan. In the region of the image where the loop-to-loop has a cusp, there are a series of light and dark bands which on the right connect to the loop-to-loop and on the left run somewhat parallel to the loop-to-loop. These apparently represent previous positions and/or configurations of the loop-to-loop formed by the anchor chain. The question often comes up as to the

HIGH-RESOLUTION MULTI-BEAM FOCUSSED SIDE SCAN SONAR

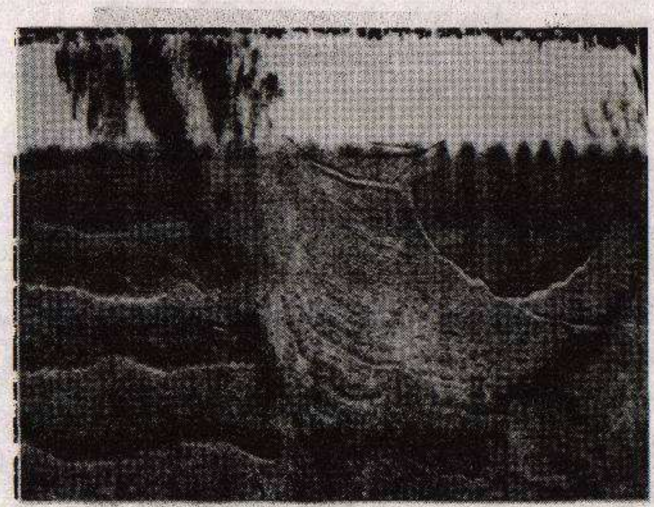

rate at which scars in surficial sediments revert to the natural scheme. High-quality seabed images, this rich with fine details, would provide valuable insight into the recovery process.

The image in figure 8 is 960 m slant range by 1200 m alongtrack and depicts a section of Trestle A of the Chesapeake Bay Bridge Tunnel near Norfolk,

Figure 7. Side Scan Sonar Image of scar pattern.

Virginia. The section has been repaired subsequent to severe damaged incurred by the impact of a large vessel. Capstones from the old bridge section and debris from the reconstruction activity lie next to the support piers. There is a lengthy shadow extending behind each of the support piers. There are also extensive shadows behind the discarded capstones.

In the upper right hand corner there are several circular objects, each with a vertical expression. These were not investigated by specific diver observation but are interpreted as tires like those which are often used by tugboats as fenders.

Figure 9 is a plywood target approximately 1.2 by 1.2 m onto which an "X" pattern has been superimposed. Thirty-eight TechSpheres, manufactured by Flotation Technologies of Biddeford, Maine, were used to make up the "X." Each of the TechSpheres is 5 cm in diameter and has a target strength of approximately -40 dB. The TechSpheres were contained in cotton socking which was attached to the plywood on either side of each TechSphere. This reference target was set on the bottom in 10 m water depth and imaged repeatedly. Whereas the nature of the circular features in figure 8 is open to interpretation, the reference target is uniquely known.

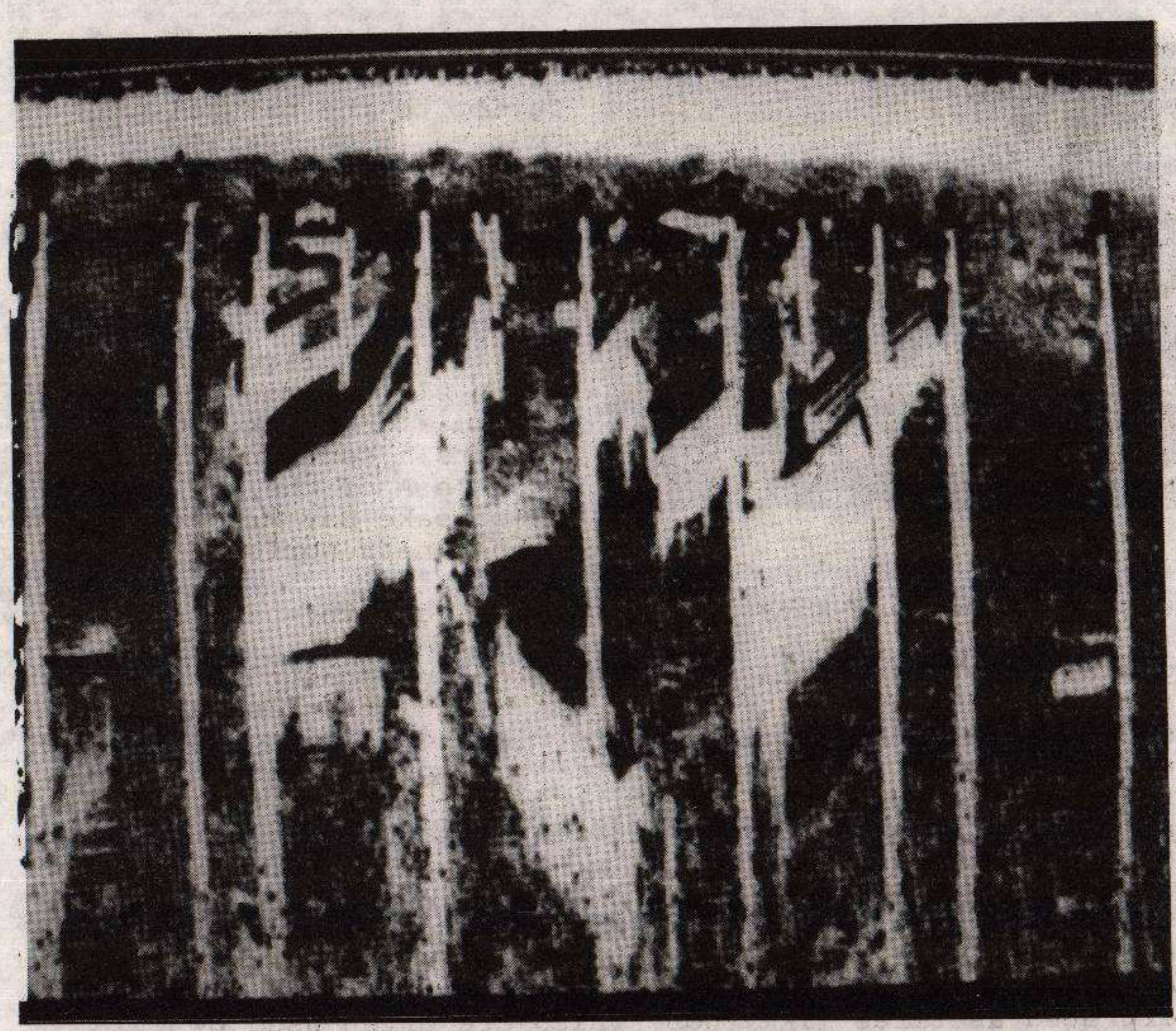

Figure 8. Side Scan Sonar Image of Chesapeake Bay Bridge Tunnel.

Figure 10 is an impressive demonstration of the high-resolution multi-beam focussed side scan sonar's imaging ability. The image with the reference target is 100 m across track by 65 m alongtrack. The reference target appears at a slant range of 70 m near the left edge of the image.

5. CONCLUSION

There are three specific areas in which a multi-beam

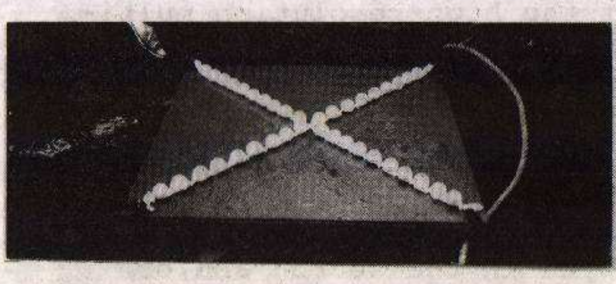

Figure 9. Reference Target.

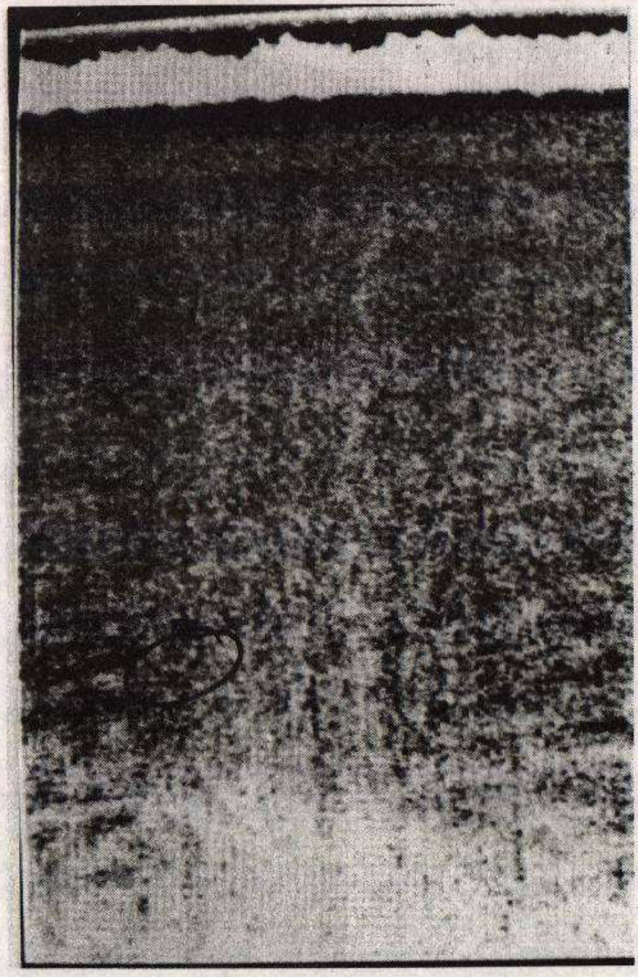

Figure 10. Side Scan Sonar Image of Reference Target.

focussed side scan sonar is superior to a conventional unfocussed single-beam side scan sonar for the pursuit of increased high-resolution area coverage. Those three areas are alongtrack resolution, alongtrack speed, and image quality. Actual field data from a prototype high-resolution multi-beam focussed side scan sonar were used to simulate the results one would have obtained using a single-beam sonar under the same conditions of crosstrack range and tow speed. It was shown that spatial aliasing of the image scene would have resulted from employing a single-beam sonar, whereas the multi-beam focussed sonar produced high-quality images.

Images from interesting targets-of-opportunity were presented that would have been difficult, if not impossible, to obtain with a conventional unfocussed single-beam side scan sonar, regardless of tow speed. Verification was not universally available for the image interpretations, however, the imaging ability of the high-resolution multi-beam focussed side scan sonar was documented through the use of a special "X" target.

The clear image obtained of that known "X" should excite side scan sonar users about the possibilities that a high-resolution multi-beam focussed side scan sonar could bring to their particular activities. Such a system is a new and valuable tool that can be employed in the search and/or identification of unique bottom features, as well as to study time and space variability of the seabed. The high-resolution area coverage rate of a high-resolution multi-beam focussed side scan sonar should improve productivity in geophysical applications and hydrography.

6. REFERENCES

Flemming, B.W., *Side-Scan Sonar : A Practical Guide*, International Hydrographic Review, Vol. LIII, No.1, January, 1976, pp 65-92.

Fox, P.A., and Denbigh, P.N., *An electronically focussed multibeam side scan sonar*, Proceedings of Acoustics and the Sea Bed Conference, University of Bath, Bath, UK, 1983, pp 347-355.

Geyer, R.A., editor, CRC Handbook of Geophysical Exploration at Sea, 2nd Edition, CRC Press, Inc., Boca Raton, Florida, 1992, pp 45-50.

Huff, L.C. and Weintroub, J., *High Speed High Resolution Side Scan Sonar - System Performance and the Impact of Phase Errors*, Proceedings of the Fourth Biennial National Ocean Service International Hydrographic Conference, Norfolk, Virginia, May 1990, pp 73-78. Reprinted in The Hydrographic Journal, No. 57, July 1990, Hydrographic Society, London, pp 19-23.

Weintroub, J. and Huff, L.C., *Preliminary Results Obtained With a Multi-Beam Focused Side Scan Sonar*, The Hydrographic Journal, No. 61, July 1991, Hydrographic Society, London, pp 11-16.

Huff, L.C. and Weintroub, J., *Field Measurements of a Multibeam Dynamically Focused Side Scan Sonar's Along Track Resolution*, Proceedings of the 1992 U.S. Hydrographic

Conference, Baltimore, Maryland, February 25-28, 1992, pp 97-102.

Lenhardt, O., *Side Scanning Sonar - A Theoretical Study*, International Hydrographic Review, Vol. LI, No.1, January, 1974, pp 61-80.

Macovski, A., *Ultrasonic Imaging Using Arrays*, Proceeding of the IEEE, Vol. 67, No.4, April 1979, pp 484-495.

Mazel C., Side Scan Sonar Training Manual, Klein Associates Inc., Salem, New Hampshire, 147 pp.,1985.

Schelkunoff, S.A., *A Mathematical Theory of Linear Arrays*, Bell. Sys. Tech. J., No.22, January, 1943, pp 80-107.

Urick, R.J., Principles of Underwater Sound, 3rd Edition, McGraw-Hill, New York, 423 pp., 1983.